Process Safety and Environmental Protection 173 (2023) 558–566

Contents lists available at ScienceDirect

Process Safety and Environmental Protection

journal homepage: www.journals.elsevier.com/process-safety-and-environmental-protection

Low-cost activated carbon from the pyrolysis of post-consumer plastic waste and the application in CO_2 capture

Ana Ligero, Mónica Calero *, Antonio Pérez *, Rafael R. Solís, Mario J. Muñoz-Batista, M.Ángeles Martín-Lara

Department of Chemical Engineering, University of Granada, 18071 Granada, Spain

ARTICLE INFO

Keywords:
Plastic waste
Char pyrolysis
Activated carbon
CO_2 adsorption

ABSTRACT

Chemical recycling by pyrolysis of plastic waste has been considered a potential approach. However, little attention has been paid to the reuse of the char residue generated. The preparation of materials from char residue obtained from the pyrolysis process has become an essential task. The purpose of this work is the preparation of activated carbons from the resulting char from the pyrolysis of a dirty and wet mixture of post-consumer plastic waste. The porous materials have been applied to the adsorption of CO_2. Both physical and chemical activation methods were investigated to modify the surface texture properties. The properties of the developed activated carbons were characterized by diverse techniques such as elemental and proximate analysis, Fourier Transform Infrared Spectroscopy (FTIR), adsorption-desorption isotherms with N_2, and Scanning Electron Microscopy (SEM). Among all synthesized samples, the activated samples prepared by chemical activation with KOH (char: KOH ratio 2:1; surface area, 487.0 $m^2 \cdot g^{-1}$) exhibited the highest CO_2 adsorption uptake (~49 $mg \cdot g^{-1}$). The activation temperature was explored within 680–840 ºC. For physical activation, an increase in the activation temperature decreases the adsorption uptake of the samples. For chemical activation, the adsorption increased as activating temperature rise to a maximum value, subsequently decreasing with further temperature rise. Increasing the amount of the chemical activating agent significantly decreases the adsorption capacities. The best-activated carbon was chosen, and several parameters were investigated on CO_2 adsorption, C: KOH mass ratio (6:1–1:4), and adsorption temperature (15–60 °C). The highest adsorption of CO_2 achieved was 62.0 $mg \cdot g^{-1}$ for activated carbon operating at the lower adsorption temperature (15 ºC).

1. Introduction

Plastics have many uses in our lives, making them easier, from drinking clean water and keeping food fresh to being part of everyday utensils and equipment such as components of our phones, cars or building materials. Plastics are versatile, durable and incredibly adaptable, and over the last century, they have offered innovative solutions to society's ever-evolving needs.

The plastics industry is essential to the economy and recovery plan in Europe. Together, producers of raw materials, plastics processors, plastics recyclers, and machinery manufacturers represent a value chain that employs more than 1.5 million people in Europe, through more than 50,000 companies operating in all European countries, generating a business turnover of over €330 billion (Plastics Europe, 2021). However, plastic pollution has become one of the most concerning environmental issues. The non-degradable nature of plastics and their fast-increasing production have to lead their rapid accumulation in the environment where they are accumulated or partially degraded into toxic by-products (Masry et al., 2021), which has caused diverse severe problems in human health and the environment (Leal Filho et al., 2019), especially to marine organisms (Mofijur et al., 2021). In 2021, 29.5 million tonnes of plastic waste were collected in Europe, 12.4 million tonnes of which were used for energy valorization, 10.2 million tonnes were recycled and 6.9 million tonnes were landfilled (Plastics Europe, 2021).

In addition to waste generation, plastics contribute to the emission of greenhouse gases measured in terms of carbon footprint throughout their useful life, from their manufacture, transport and use until their waste disposal (Cabernard et al., 2021). The governments of developed countries are currently working on plastics to tackle plastic pollution and reduce marine litter, accelerating the transition into a circular plastics economy. In particular, the European Union, through the European Green Deal, has proposed no net emissions of greenhouse gases

* Corresponding authors.
E-mail addresses: mcaleroh@ugr.es (M. Calero), aperezm@ugr.es (A. Pérez).

https://doi.org/10.1016/j.psep.2023.03.041
Received 21 February 2023; Received in revised form 15 March 2023; Accepted 15 March 2023
Available online 17 March 2023

by 2050 (European Comission).

In this context, the chemical recycling of plastic waste by pyrolysis is considered an attractive technology for reducing plastic waste and greenhouse gas emissions, as well as promoting the circular economy (Chen et al., 2021; Thiounn and Smith, 2020). Nowadays, a small fraction of plastic waste is mechanically recycled. However, a great amount of plastic waste, either mixed or contaminated, cannot be easily recycled by mechanical methods without an intensive and expensive pre-treatment that reduces the technical and economic viability of the process (Solis and Silveira, 2020). Therefore, some interesting thermochemical procedures such as pyrolysis are being examined (Chao-Hsiung et al., 1993; Jaafar et al., 2022; Williams and Slaney, 2007; Williams and Williams, 1998). Nowadays, major chemical companies are promoting pyrolysis plants for converting mixed plastic waste into hydrocarbon feedstocks.

Regarding the applicability of products from the pyrolysis of plastics, the use of liquid and gas fractions has been developed to a great extent over the years for the recovery of compounds and energy production (Al-Salem et al., 2020; Santos et al., 2018; Zhang et al., 2020). However, the applications for the solid residue, known as char, have been less explored, and, in most plants, roughly 1–10% of the product is char. The char is sent to the landfill or can be used in the production of asphalt or concrete (Zhang et al., 2018; Zhao et al., 2014). Recently, some new uses have been explored. For example, it has been used as a precursor, producing activated carbons for application in diverse areas including wastewater treatment and gas separation, among others (Ge et al., 2016; Li et al., 2020; Martín-Lara et al., 2021; Yuan et al., 2020). The objective of the present work is the preparation of activated carbons from the resulting char obtained after the pyrolysis of a post-consumer contaminated mixture of plastic waste that came from the rejected fractions of a local municipal solid waste treatment plant. The char was activated and the performance of CO_2 adsorption was studied. The effect of the preparation method on the characteristics and CO_2 adsorption capacities has been deeply investigated, considering different chemical activator agents, the temperature of activation, and the ratio between char and activated agent. To our knowledge, no studies have been reported on the development of activated carbons from char of pyrolysis obtained of real mixtures from municipal plastic waste collected from rejected fractions without any manipulation or pre-treatment. Most published works use simulated mixtures of pure materials or single polymer types such as polyethylene terephthalate.

2. Materials and methods

2.1. Char production by pyrolysis

The char was obtained from the pyrolysis of contaminated and mixed plastic waste provided by a municipal solid waste (MSW) treatment plant located in the province of Granada (Spain). The rejected fraction of mixed plastic from the MSW included polypropylene (PP); polystyrene (PS), either as high impact PS (HIPS) or expanded PS (EPS); and film, mainly polypropylene. Firstly, manual classification and quantification of the mixed plastic were carried out to determine the average composition of the polymers, resulting in the mass content being PP (55%) PS (8.6%), EPS (10.1%) Film, (27.7%). The mixture was crushed to a particle size lower than 1 mm.

Based on the experience of previous research (Idrees et al., 2018), a pyrolysis experiment was carried out in a reactor system that consists of a tubular furnace under a flow rate of N_2 50 $L{\cdot}h^{-1}$, a residence time of 90 min, a heating rate of 50 $^{o}C{\cdot}min^{-1}$ and operating temperature of 500 °C. Under these conditions, the following product yields were obtained: liquid (oil) 57.3%, solid (char) 6.2%, and gas 36.5%. The resulting char, referred to as 'C', was ground and subsequently activated to produce the activated carbons by both physical and chemical activation methods. Also, the char was cleaned with 1 $mol{\cdot}L^{-1}$ HCl and dried at 120 °C for 24 h, labeled as 'TC'.

2.2. Char activation

For physical activation, a thermal three-step process was carried out under an inert atmosphere, 200 $mL{\cdot}min^{-1}$ of N_2 or CO_2. Firstly, 5 g of char was heated from room temperature to the target value (680, 720, 760, 800, or 840 °C) at a rate of 10 $^{\circ}C{\cdot}min^{-1}$. Next, the sample was submitted to a flow of N_2 or CO_2, holding this temperature for 1 h. Finally, the sample was cooled under the same N_2 flow until room temperature. The resulting sample activated with N_2 was labeled as AC-N_2 and the sample that was treated under CO_2 as AC-CO_2. For chemical activation, 5 g of C was mixed with the activating agent, i.e., NaOH or KOH, at a chosen ratio. A five-step activation process was then carried out under an inert atmosphere, 200 $mL{\cdot}min^{-1}$ of N_2. Firstly, the solid (char and activating agent) was mixed and heated from ambient temperature to 300 °C at a heating rate of 10 $^{\circ}C{\cdot}min^{-1}$. Next, the temperature was kept for one hour at 300 °C under the same flow rate of N_2 for melting the activating agent. Then, the temperature was risen from 300 °C to the target value (680, 720, 760, 800, 840 °C) at a rate of 10°C$\cdot min^{-1}$. Next, the temperature was kept for 1 h at the selected temperature; and finally, the sample was cooled to room temperature. After activation, either for physical or chemical activation processes, the prepared materials were washed with 1 M HCl and dried at 120 °C for 24 h.

2.3. CO_2 adsorption tests

The CO_2 adsorption tests were carried out in a thermogravimetric analyzer (Perkin-Elmer, STA 6000) following three steps. Firstly, a drying step was conducted. During this step, moisture and other species that may be physisorbed onto the surface of the sample were removed. The sample was heated from room temperature to 200 °C, at which temperature the sample was kept for approximately 1 h, under an inert atmosphere, i.e. flow rate of N_2 of 50 $mL{\cdot}min^{-1}$. Secondly, a cooling step was carried out. The sample was cooled from 200 °C to a desired value for the adsorption process (15, 30, 45, and 60 °C) under an inert atmosphere, i.e. flow rate of N_2 of 50 $mL{\cdot}min^{-1}$. Finally, the isothermal CO_2 adsorption step of the dried sample was conducted. At this point, the flow rate of N_2 was changed to 50 $mL{\cdot}min^{-1}$ of CO_2 and kept for 2 h, until a constant sample mass is reached. In this step, there was an increase in mass due to CO_2 adsorption, so the difference between the initial mass of the dried sample (at the end of the cooling stage) and the obtained final mass (at the end of the isothermal adsorption step) let the determination of the CO_2 adsorbed.

2.4. Characterization of the prepared samples

The elemental analysis was carried out to determine the content of carbon, hydrogen, nitrogen, and sulfur. Oxygen was determined by the difference between the total with the other elements. A Thermo Scientific Flash 2000 device was used.

The proximate analysis was used to establish the percentage of moisture, volatiles, and ash present in the different prepared materials. The percentage of fixed carbon was determined by the difference. The quantification of the proximate analysis was carried out by thermogravimetric analysis (TGA) on a Perkin-Elmer STA 6000 thermobalance. For this procedure, 20–30 mg of solid sample was kept for 10 min at 30 °C in an inert gas atmosphere using an N_2 flow rate of 20 $mL{\cdot}min^{-1}$. The sample was then heated in a temperature range of 30–110 °C, at a rate of 40 $^{o}C{\cdot}min^{-1}$. The temperature was kept at 110 °C for 10 min. Then, the temperature was risen to 875 °C (heating rate of 40 $^{o}C{\cdot}min^{-1}$) and then kept at 875 °C for 10 min. Finally, the gas was switched to oxygen with a flow rate of 20 $mL{\cdot}min^{-1}$, and the temperature at 875 °C was kept for another 10 min. The determination of each of the constituents (moisture, volatiles, and ash) was completed by quantifying the weight loss in each step.

FTIR was conducted in a Perkin-Elmer spectrophotometer, model

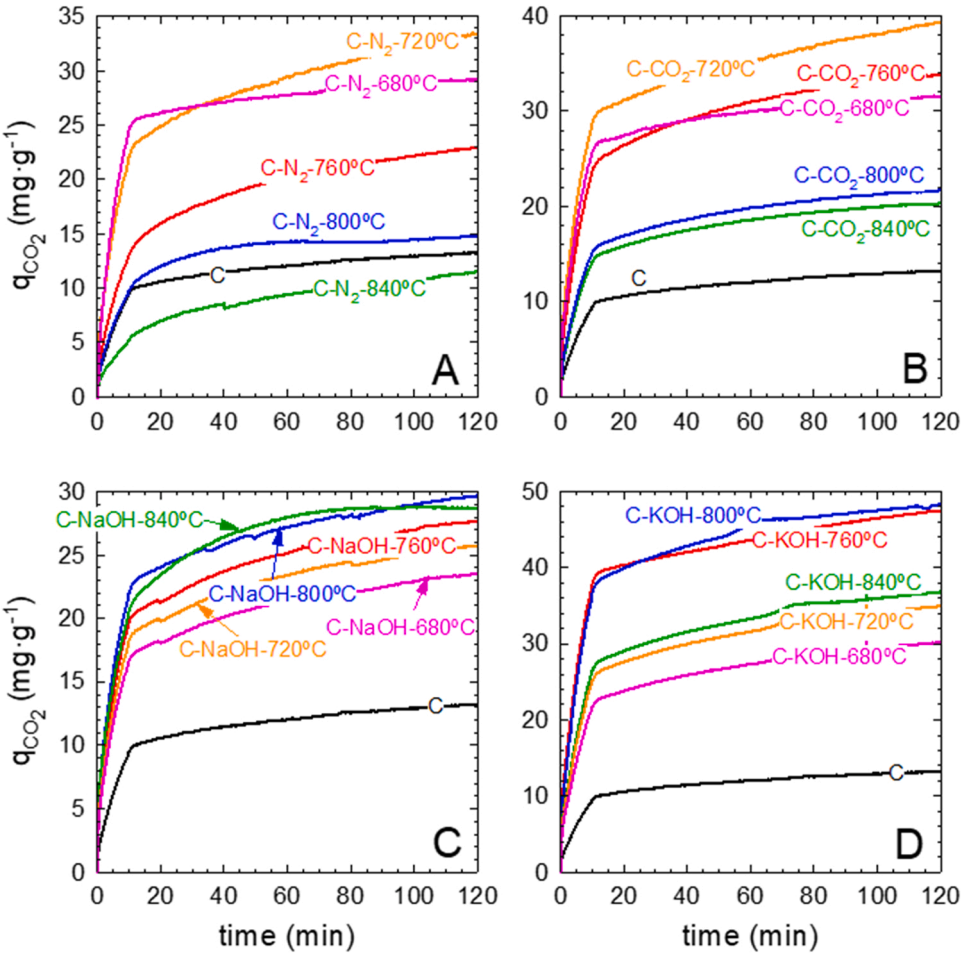

Fig. 1. Influence of the adsorption time under different methods and activators on the CO_2 adsorption performance. A) physical activation with N_2; B) physical activation with CO_2; C) chemical activation with NaOH; D) chemical activation with KOH.

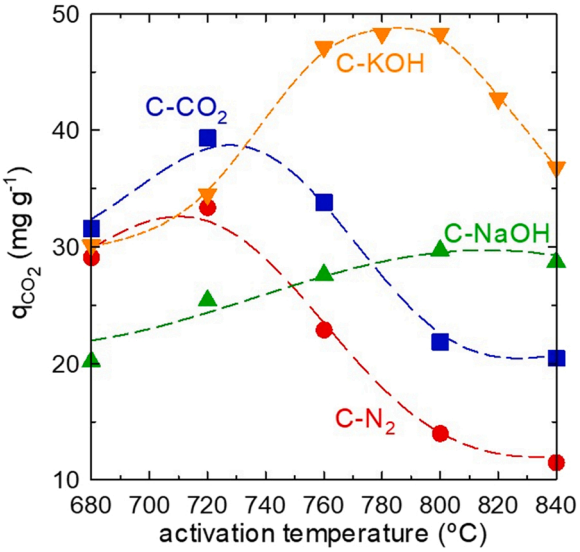

Fig. 2. Influence of the activation temperature on CO_2 adsorption performance with char samples activated and a char: agent mass ratio of 1:1.

Spectrum-65, equipped with an Attenuated Total Reflectance (ATR) device. Each spectrum was obtained in a wavelength number within 4000–400 cm^{-1} with a 0.5 cm^{-1} spectral resolution.

The textural properties were analyzed by adsorption-desorption N_2 isotherms at 77 K in an ASAP 2010 Micromeritics equipment. The total specific surface area was calculated by the BET method (S_{BET}) and the total pore volume was determined from the N_2 uptake at p/p_0~0.99. The t-plot method was used for the estimation of the specific surface of micropores (S_{MP}) and the volume of micropores (V_{MP}). The average pore size was obtained by the BJH method from the adsorption step.

The morphological properties of the samples were analyzed by SEM with Energy Dispersive X-ray (EDX) analysis in an Auriga (FIB-FESEM) device.

3. Results and discussion

3.1. CO_2 adsorption tests

3.1.1. Influence of agent type and activation temperature

Fig. 1 shows the CO_2 adsorption results as a function of contact time for the different activation techniques (physical and chemical) and activation temperatures of 680, 720, 760, 800, and 840 ºC. For chemical activation methods a char: agent mass ratio of 1:1 was used.

The results show that both physical and chemical activations are effective alternatives. The CO_2 adsorption uptake obtained with the activated materials improved in all cases if compared to the char. Regarding the effect of activating temperature, see Fig. 2, for physical activating methods, the adsorption results increased slightly when the temperature increased from 680 ºC to 720 ºC to gradually decrease with further increase of the activation temperature, obtaining values between 11.5 and 33.4 $mg{\cdot}g^{-1}$ for N_2 and between 20.4 and 39.3 $mg{\cdot}g^{-1}$ for CO_2,

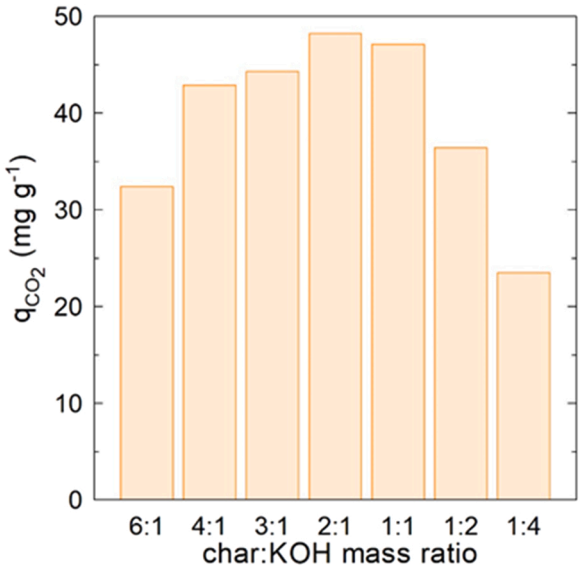

Fig. 3. Influence of char: KOH mass ratio on CO_2 adsorption uptake.

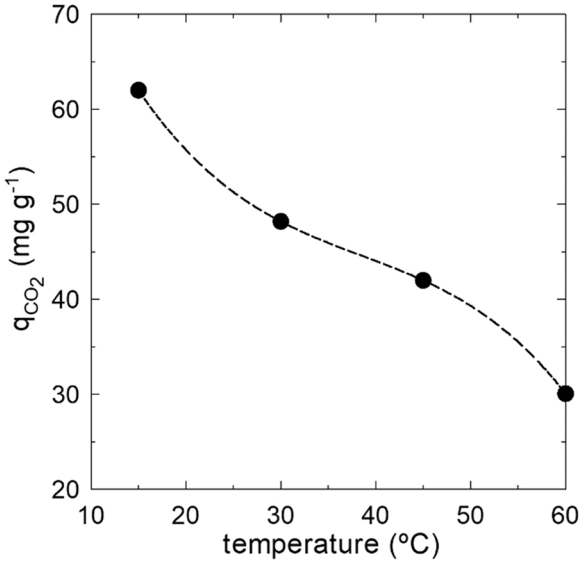

Fig. 4. Influence of the adsorption temperature on the CO_2 adsorption with C-KOH at 760 °C at a char: KOH dose of 2:1.

with the maximum values reached at 720 °C. Similar results were achieved in the activation of oil palm shells with N_2 and CO_2, being the best adsorption results obtained when materials were prepared at low temperatures, close to 750 °C (Hoseinzadeh Hesas et al., 2015). However, the adsorption values obtained by these researchers were much higher than this work, i.e., the order of 186 mg·g^{-1} for activation with CO_2 and 132 mg·g^{-1} for activation with N_2, possibly since the activation was enhanced by the microwave technique and the carbon precursor had a biomass source. The decreasing CO_2 adsorption uptake with the rise of the activation temperature was also observed when treating commercial activated carbon with N_2, H_2, and ammonia (Zhang et al., 2010). Also, the reported CO_2 adsorption uptake after the activation with N_2 was higher than this work, possibly due to the precursor material nature, which was an activated carbon with a high previous porosity developed if compared to the char of the pyrolysis of this work. The negative impact of the activation temperature on adsorption capacities has been also reported in the activation of polyacrylonitrile (PAN) for the adsorption of CS_2 in gaseous streams (Li et al., 2020). A collapse and the release of polycondensation reactions were attributed to a lesser adsorption ability as the microporosity dramatically decreased by raising the temperature to over 700 °C. It has been reported that the interaction between CO_2 and carbon adsorbents is enhanced in the presence of micropores (< 1 nm) (Ge et al., 2019).

The chemical activation method led to improved CO_2 adsorption capacity if compared to the physical method, mainly at high activation temperatures. Either in the presence of NaOH or KOH, an initial increase in the activation temperature from 680 to 800 °C led to an increase in CO_2 adsorption uptake. Nonetheless, a further increase in the activation temperature produced different results depending on the alkali used. A further rise of the activation temperature to 840 °C did not significantly modify the CO_2 adsorption uptake when using NaOH (27.6 and 29.7 mg·g^{-1}) while a considerably negative effect was registered with KOH reducing the CO_2 adsorption from 48.3 to 36.8 mg·g^{-1}. Similar conclusions regarding the behavior of CO_2 adsorption over the activation temperature for both activating agents and the advantage of using KOH over NaOH have been reported (Ge et al., 2016; Yuan et al., 2020). KOH is more effective than NaOH to develop higher microporosity that is negatively affected by a risen temperature (Adibfar et al., 2014; Almazán-Almazán et al., 2007; Yuan et al., 2020). Higher CO_2 adsorption uptake was also reported in the literature with activated chars obtained from pure plastics. The activation of char obtained from the pyrolysis of polyethylene terephthalate (PET) with KOH was than NaOH for CO_2 adsorption, uptake of 194.5 mg·g^{-1} at 25 °C for PET-KOH and 169.8 mg·g^{-1} at 25 °C for PET-NaOH (Yuan et al., 2020). The effect of activation with NaOH and KOH was also studied with char generated from polyurethane foam waste. The resulting material was reported as very efficient also for CO_2 capture. KOH led to higher CO_2 uptake values than those found with NaOH, reaching a maximum of 257.4 mg·g^{-1} at 0 °C (Ge et al., 2019).

Although physical activation has a lower environmental impact as no chemical reagents such as KOH or NaOH are used, the application of KOH as the activating agent seems to be the best option to prepare activated carbons from a mixture of plastic waste focused on CO_2 adsorption. From Fig. 2a maximum CO_2 uptake close to 49 mg·g^{-1} within 760–800 °C is observed for KOH. As the differences in this range are minimal, the lower value, i.e., 760 °C, was chosen due to an energy-saving aspect.

Table 1
Elemental analysis of the selected activated char samples.

Sample	Activation temperature	C:agent ratio	Percentage (%)				O/C ratio
			N	C	H	O[a]	
C	-	-	0.86	35.62	2.23	61.29	1.72
TC	-	-	1.72	45.16	2.47	50.65	1.12
C-N_2	720	-	1.11	43.55	0.97	54.37	1.25
C-CO_2	720	-	1.23	51.17	0.78	46.82	0.91
C-NaOH	800	1:1	0.33	16.89	1.59	81.19	5.03
C-KOH	760	2:1	0.72	28.76	0.86	69.66	2.42
C-KOH	760	6:1	0.78	41.12	1.15	56.95	1.38

[a] Obtained as the difference.

Table 2
Proximate analysis of the activated char samples.

Sample	Activation temperature	C:agent ratio	Percentage (%)			
			Moisture	Volatile	Ash	Fixed carbon
C	-	-	3.10	27.89	46.21	22.81
TC	-	-	2.73	27.77	33.38	36.12
C-N_2	720	-	2.89	10.37	40.51	46.23
C-CO_2	720	-	1.80	8.22	42.07	47.91
C-NaOH	800	1:1	4.29	25.58	58.90	11.23
C-KOH	760	2:1	2.48	11.89	66.01	19.62
C-KOH	760	6:1	5.30	18.13	42.73	33.82

Table 3
Textural properties from the N_2 adsorption-desorption isotherms of the activated char samples.

Sample	Activation temperature	C: agent Ratio	S_{BET} ($m^2 \cdot g^{-1}$)	S_{MP} ($m^2 \cdot g^{-1}$)	V_T ($cm^3 \cdot g^{-1}$)	V_{MP} ($cm^3 \cdot g^{-1}$)	V_{MP}/V_T (%)	Pore size (Å)
C	-	-	14.7	0.8	0.025	-	-	66.2
TC	-	-	19.3	0.1	0.040	0.036	90.0	81.2
C-N_2	720	-	48.4	0.0	0.155	0.000	0.0	128.3
C-CO_2	720	-	100.0	22.6	0.209	0.011	5.3	82.5
C-NaOH	800	1:1	246.9	184.9	0.217	0.084	38.9	71.6
C-KOH	760	2:1	487.0	414.2	0.300	0.180	60.0	54.4
C-KOH	760	6:1	295.3	210.3	0.236	0.093	39.4	59.9

S_{BET}: total specific surface area by BET method; S_{MP}: micropore surface area; V_T: total pore volume; V_{MP}: micropore volume. Average mesoporous diameter (4 V/A) by the BJH method from the adsorption step

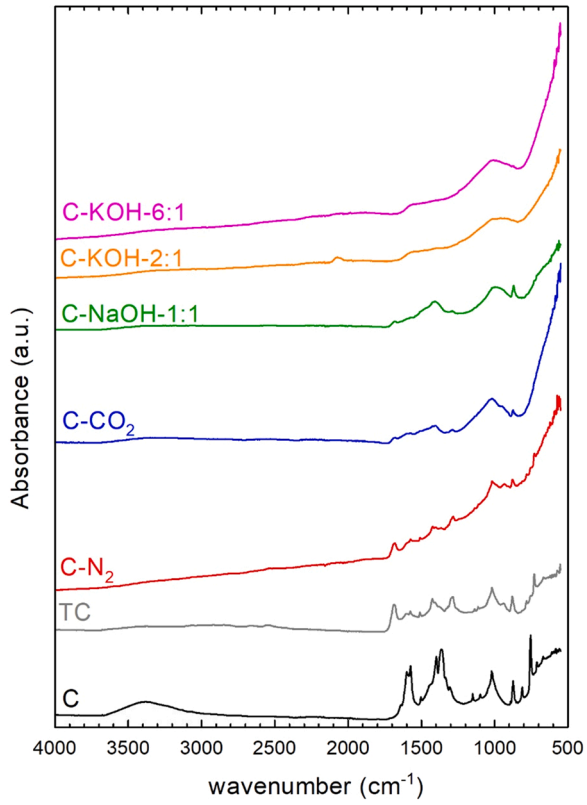

Fig. 5. FTIR spectra of the activated char samples.

3.1.2. *Influence of the char: KOH mass ratio*

Due to the better results achieved using KOH, this activating method was further investigated by varying the ratio char: KOH fixing the temperature at the optimum value, i.e., 760 ºC. Fig. 3 shows the CO_2 adsorption capacities of the prepared materials with different char: KOH mass ratios.

The activated materials prepared with a char: KOH mass ratio lower or equal to 1:1 showed a lower CO_2 adsorption uptake. This behavior can be explained by a lack of KOH for an efficient definition of a well-developed microporosity structure, being the amount of alkali insufficient (Ge et al., 2016; Idrees et al., 2018; Kaur et al., 2019a). This could suggest that an increase in the mass of the char could produce an improvement in CO_2 adsorption; however, for char: KOH mass ratios higher than 2:1 the adsorption uptake also decreased and, for a very high char: KOH, i.e. 6:1, the adsorption uptake fell to 32.4 $mg \cdot g^{-1}$ regarding the optimum value found for a char: KOH ratio of 2:1. At moderate char: KOH a mass ratio, this action is increased until an optimum is reached. Nevertheless, if the amount of KOH is risen the evolution of micropores by the excessive attack of the KOH to mesopores takes place. Therefore, since the micropores are responsible for CO_2 adsorption due to their more appropriate size, there is a decrease in CO_2 adsorption. This effect was registered when raising the amount of KOH, being this effect more negative in relative proportions than the rise of char amount. The optimum value was observed with a char: KOH ratio of 2:1. This proportion is in good agreement with other works although the char used in this study is a mixture of plastics. A ratio char: KOH ratio of 3:1 was obtained as the optimum when using PAN (Singh et al., 2019). The char from polystyrene foam filler led also to an optimum ratio of 3:1 (Idrees et al., 2018). The activation of polyurethane foams led to a 1:1 optimum (Ge et al., 2016). The activation of the char from polyethylene terephthalate has been also reported as optimum at a 3:1 ratio (Kaur et al., 2019b, 2019a).

3.1.3. *Influence of the adsorption temperature*

After the selection of KOH as the activating agent, 760 ºC as the optimum temperature, and 2:1 as the best char: KOH ratio, the influence of the temperature during the CO_2 adsorption was analyzed, see results in Fig. 4. According to the results depicted in this figure, the CO_2 uptake decreased with a rise in the temperature obtaining a maximum value of 63 $mg \cdot g^{-1}$ at 15 ºC and a minimum value of 30 $mg \cdot g^{-1}$ at 60 ºC. A similar trend was observed at adsorption temperatures between 25 ºC and 75 ºC by other researchers for adsorbent materials prepared from PET waste that were also chemically activated with KOH (Yuan et al., 2020). Also, this negative effect has been reported by other authors (Ge et al., 2019; Idrees et al., 2018; Kaur et al., 2019b; Singh et al., 2019). For example, the CO_2 adsorption of char from packaging waste activated

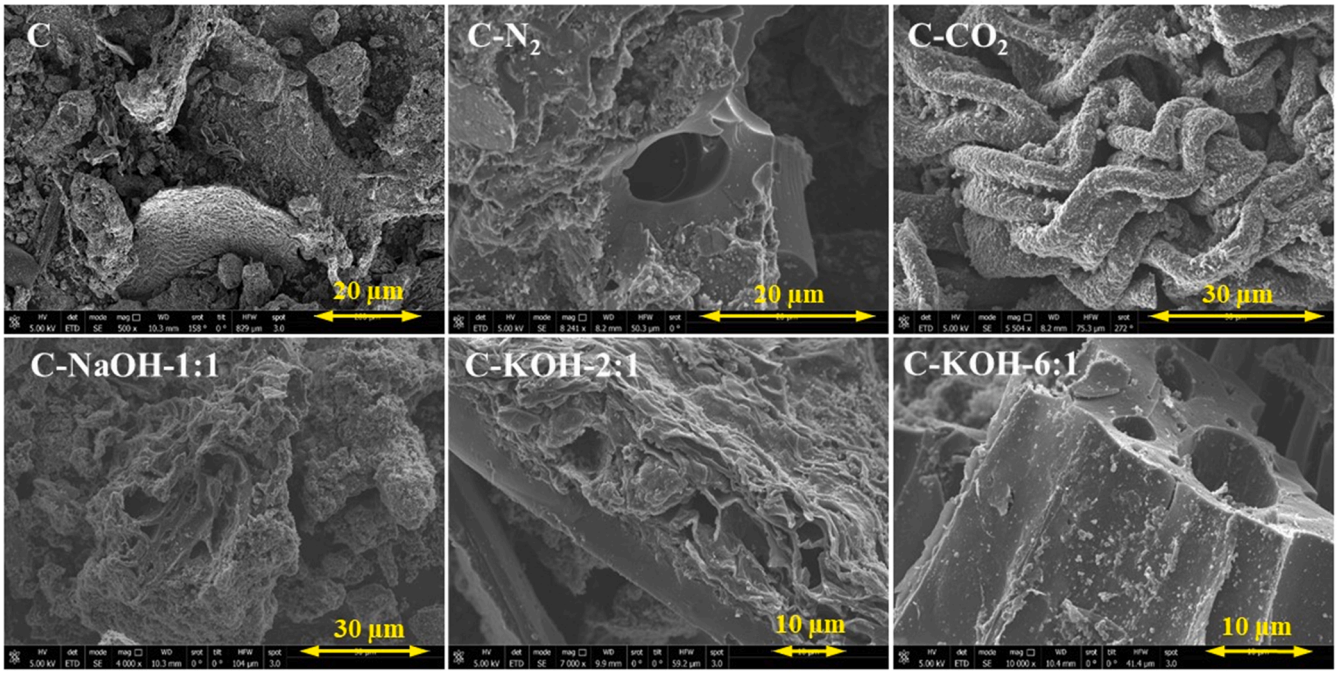

Fig. 6. SEM pictures of the activated char samples.

with KOH led to a decrease of CO_2 uptake from 133.7 $mg \cdot g^{-1}$ to 38.7 $mg \cdot g^{-1}$ when rising the temperature from 0 °C to 50 °C (Idrees et al., 2018). In the activated char prepared from polyacrylonitrile with KOH also has been reported this negative effect of the temperature, with CO_2 uptakes decreasing from 110 to 35.2 $mg \cdot g^{-1}$ by raising the temperature from 30 to 100 °C (Singh et al., 2019). Besides, the resulting material from char made of PET after activation also leads to a negative effect on CO_2 uptake (Kaur et al., 2019b).

The rise of the adsorption temperature is associated to an increase in the mobility of CO_2 molecules in the adsorbate; therefore, the molecular diffusion effect is connected. This aspect joined with the fact that CO_2 adsorption is a physisorption process, causes even more agitation, so the molecular diffusion rate and surface adsorption energy could increase, thus resulting in the instability among CO_2 molecules leading to lower adsorption values (Guo et al., 2021; Shi and Liu, 2021; Wu et al., 2021).

3.2. Characterization of the activated chars

The different activated carbons prepared under different activation methods that presented better CO_2 adsorption performance were chosen for complete characterization. For such a purpose, the following activation agent char: alkali ratio at their optimum activation temperatures were selected, N_2-720, CO_2-720, NaOH-1:1–800, KOH-2:1–760. Also, the activated carbon was prepared by chemical activation with KOH but with the lowest cost in terms of using the lowest KOH dose at the lowest temperature, which means the sample KOH-6:1–760, as well as the precursors' materials, untreated char, and treated char, were characterized.

3.2.1. Elemental and proximate analysis

The results obtained in the elemental analysis are reported in Table 1. As can be expected in the case of plastic precursors, the N content is negligible over carbon, hydrogen, and oxygen, because of their hydrocarbon-derived origin. The high oxygen content can be attributed to the carbonization process and the decomposition of volatile compounds (Panahi et al., 2021). It is observed that the treatment of the char with HCl decreased the content of oxygen due to the removal of oxygenated functional groups, which led to a C content increment. The physical activation with N_2 and CO_2 increased led to very similar results if compared to the treated sample. Regarding the chemical activation process, the highest carbon content was found for the KOH-activated sample, char:KOH ratio 6:1 at 760 °C, and the lowest for the NaOH-activated sample, char:NaOH ratio 1:1 at 800 °C. This may be caused by the higher temperature used in the activation process. However, it has been reported that KOH displays better performance as it is less influenced by the temperature in terms of carbon yields if compared to NaOH when activating a char from the pyrolysis of PET (Almazán-Almazán et al., 2007). At high temperatures as 800 °C, NaOH can contribute to the reaction of the solid carbon of char which can lead to an increase in the inorganic content of the generated activated carbon as confirmed by the high ash content of this sample.

The O/C ratios were higher in the chars activated with the alkalis. The decomposition of the metal hydroxide into oxides within the carbon matrix contributed to the enhancement of the oxidation (Chen et al., 2020; Park and Jung, 2002), explaining why the higher ratio of KOH led to the higher oxygenated content after activation.

Table 2 shows the proximate analysis results of the selected materials. In general, low moisture content and high ash contribution were registered. If the untreated and treated samples are compared, the ash content decreased after the acidic wash. The HCl washing process contributed to removing part of the inorganic matter of the material (Kozyatnyk et al., 2021). The ash content increased after the activation process, probably due to the release of volatile compounds, concentrating the non-volatile content as ash. The activation with KOH led to the highest ash content due to the high ability to burn the material, followed by NaOH. There is a compromise between the carbon content and the microporosity. Therefore, although during the activation the formation of micropores is desired, excessive and uncontrolled reactions of combustion would lead to low carbon and high ash content.

3.2.2. N_2 adsorption/desorption isotherms

The textural results of N_2 adsorption-desorption isotherms are summarized in Table 3. The char displayed a very low surface area, 14.7 or 19.3 $m^2 \cdot g^{-1}$ before and after HCl washing, respectively. The thermal treatment improved the textural properties. The microporosity order in terms of specific surface area and micropore volume observed was N_2

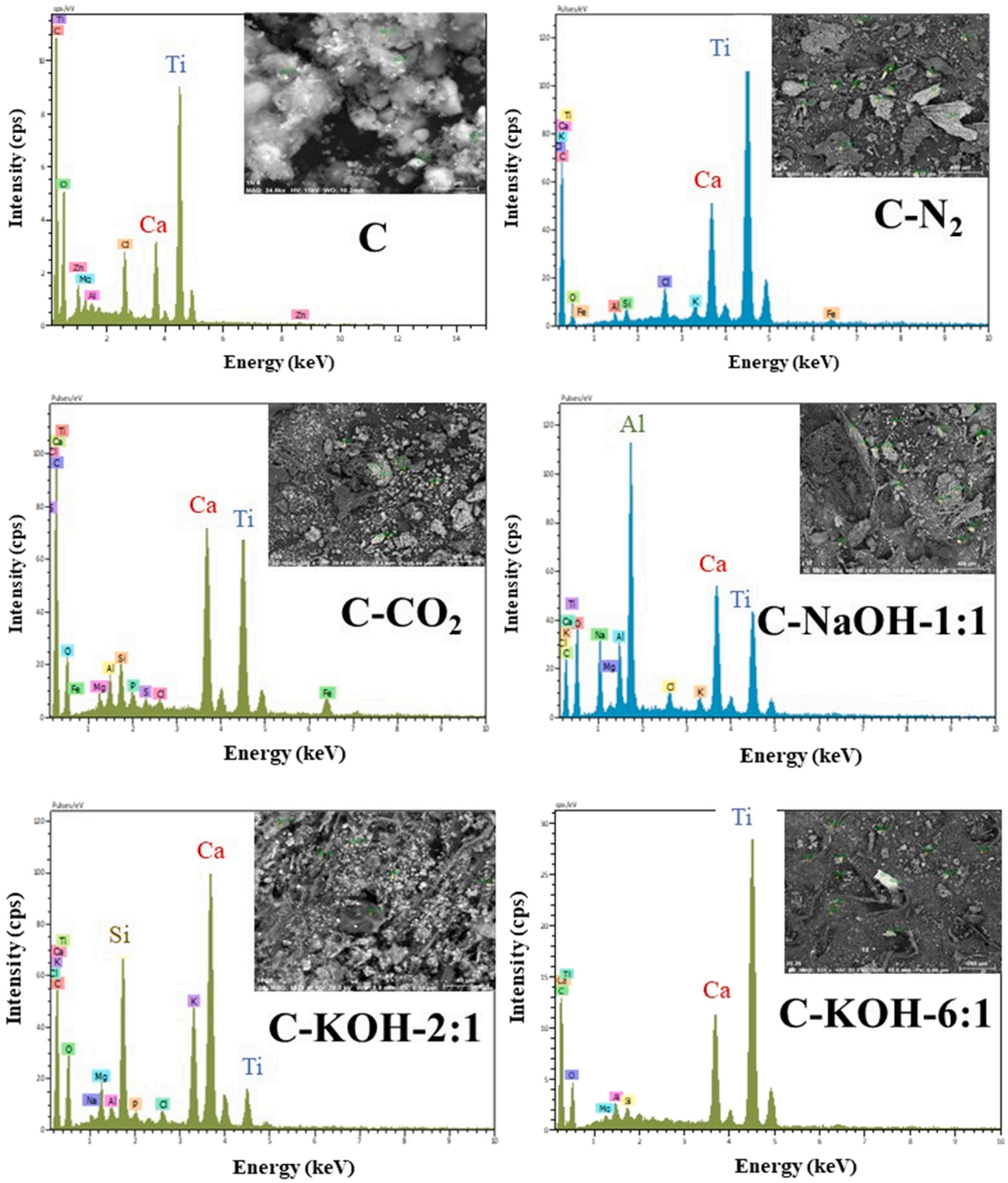

Fig. 7. Multipoint EDX analysis of the activated char samples.

$<CO_2$ <NaOH<KOH, obtained at their optimum activation temperatures. From these results, it can be observed that the chemical activation methodology with the hydroxides is preferred to the physical process, since it led to a considerable increase in the specific surface area, in the case of KOH higher than NaOH, as reported in the literature (Almazán-Almazán et al., 2007). The reaction developed during the activation with both hydroxides is very similar, involving the formation of hydrogen, carbonates, and alkali metals or alkali oxides. However, the main difference between the two activation agents is the temperature at which these reactions are released, being lower in the case of KOH (Lillo-Ródenas et al., 2003). KOH is preferred for the development of microporosity whereas NaOH is convenient for controlling mesoporosity (Tseng, 2006). Consequently, the use of KOH at a 2:1 ratio led to the best textural properties, a BET surface area of 487.0 $m^2 \cdot g^{-1}$, micropore surface area of 414.2 $m^2 \cdot g^{-1}$, and micropore volume of 0.180 $cm^3 \cdot g^{-1}$, which would explain the best CO_2 adsorption uptake since the microporosity, rather than mesoporosity, is essential to enhance CO_2 adsorption yield (Ge et al., 2016). The average pore size obtained also provides evidence of the generation of mesopores of smaller size in the case of the activation with KOH vs NaOH. A decrease of the KOH proportion, i.e. char:KOH ratio of 6:1, led to a lower microporosity property which results detrimental to the CO_2 adsorption.

3.2.3. *Fourier transform infrared spectroscopy (FTIR) analysis*

Fig. 5 depicts the FTIR spectra of the activated chars. The char precursor exhibited a wide band within 3000–3700 cm^{-1}, attributed to the HO stretching of water, phenols, and alcohols (Wang et al., 2017). In the lower wavelength number region, diverse peaks were registered. The

presence of a band around 1600 cm^{-1} can be ascribed to the stretching of C═C or quinolinic C═O (Duranoğlu and Beker, 2012). Moreover, the peaks located at 1383 cm^{-1} are associated with the superposition of -OH and -CH functional groups (Rashidi et al., 2021). Intense peaks at 1584 cm^{-1} and 1090 cm^{-1} associated with C-O stretching were also observed (Ge et al., 2019). The presence of bands around 1000 cm^{-1} indicates the presence of oxygenated functional groups, which favor the adsorption of CO_2, by Van der Waals interaction, due to the electronegative character conferred to the surface (Kaur et al., 2019a). The remaining bands concentrated around 550 cm^{-1} and 750 cm^{-1} can be attributed to the stretching of the aromatic C═C bonds (Bedin et al., 2016). Furthermore, the presence of oxygenated moieties enhances the Lewis basic character of the carbons which is favorable for the adsorption of acidic CO_2.

The spectrum of the treated char lacks the wide band centered at 3500 cm^{-1} of hydroxylated groups, because of the HCl cleaning. A peak at 1380 cm^{-1}, associated with the asymmetric vibration of the -COO group (Ge et al., 2019), and a peak at 1425 cm^{-1} assigned to C═C vibrations in aromatic rings (Panahi et al., 2021) was defined in the TC sample but at lower intensity compared to the native char. The peak at 1000 cm^{-1} due to the presence of oxygenated groups was kept after HCl cleaning. The intensity of the C═C peak at 750 cm^{-1} disappeared in the TC sample probably due to the stabilization with HCl washing.

The physical treatment with N_2 kept the fingerprint of the treated char, decreasing significantly the intensity of the peaks, probably due to the release of superficial volatile compounds (Rashidi et al., 2021). If CO_2 was used for the activation, almost all the peaks were removed except for a wide peak attributed to the hydroxylated groups at 1000 cm^{-1}. The chemical activation either with NaOH or KOH led to the removal of the original FTIR peaks of the treated char, defining a wide peak located at 1000 cm^{-1}, attributed to hydroxylated groups that were more intense in the case of KOH.

3.2.4. Scanning electron microscopy (SEM)

Some SEM micrographs of the activated char are shown in Fig. 6. The pictures collected in each material considerably vary in the same sample due to the displayed heterogeneity. However, the images most representative have been selected. In general terms, the porosity developed can be correlated with the textural properties, leading to more rugosity and cavities in those samples with more surface areas. The morphology of the original and treated char was not porous, depicting the shape of sheets or filament-like structures.

In the case of N_2 activation, a smooth lamellar structure was observed. The sample activated with CO_2-720, developed certain rugosity on the surface, which provides evidence of the higher surface area compared to N_2 activation. The activation with NaOH led to a more compact and rougher structure, with a predominance of larger pores, although smaller pores are also envisaged. The activation with KOH led to a very different structure. The activation with a char:KOH ratio of 2:1 produced a layered structure that shows numerous pores created by the overlapping of the layers. However, with the ratio of 6:1, a tubular block structure was obtained, with a solid, smooth consistency that forms larger pore sizes. The formation of porous channels in the presence of alkaline hydroxides over the smoothed precursor char has been already reported in previous works dealing with PET (Adibfar et al., 2014; Kaur et al., 2019a, 2019b), polyurethane (Ge et al., 2019, 2016), or polyacrylonitrile (Li et al., 2020; Singh et al., 2019). Also, EDX analysis was used to analyze the nature of the compounds present in the different samples, see Fig. 7. Due to the heterogeneity of the samples, diverse punctual analyses were carried out to obtain an average value of the composition. The presence of C and O was common in all the plastic compounds. In addition, some metallic elements were detected. For example, an abundant presence of Ca and Ti was observed in all samples, probably due to the presence of CaO and TiO_2 in the pyrolyzed plastics, as both elements are common additives widely used in the manufacture of plastic materials to improve the mechanical properties (CaO) or as a white pigment (TiO_2) (Martín-Lara et al., 2021). The presence of other metals such as Al or Si can be associated with the origin of the plastic, obtained from municipal waste as reported in the literature (Cansado et al., 2022).

4. Conclusions

This work provides a study about the valorization of a char obtained in the pyrolysis of a mixture of real plastic from the fraction rejected in a recycling plant. The activation temperature highly affects the CO_2 adsorption uptake. The physical activation, i.e. N_2 or CO_2, displayed their maximum CO_2 uptakes at 720 ºC, whereas chemical activation required higher temperatures, i.e. 760 ºC for KOH and 800 ºC for NaOH. Between physical (N_2 and CO_2) and chemical (NaOH and KOH) activation, the chemical treatment with alkali hydroxide resulted in the best alternative to develop a porous material. The use of KOH was more effective than NaOH. Also, the ratio char:KOH was optimized, observing the highest performance of CO_2 uptake with a value of 2:1, with a value of approximately 49 $mg{\cdot}g^{-1}$. The effect of the operating temperature during the adsorption tests has a negative impact, decreasing with a rise in the temperature due to molecular diffusion and surface adsorption energy effects. The textural characterization of the different activated chars corroborated the higher microporosity of the optimized material, in terms of surface area and pore volume improvement, determining factors for higher CO_2 adsorption.

The obtained results demonstrate the feasibility of the valorization of a char, a waste obtained during the chemical recycling of plastics via pyrolysis. The char can be used as a feedstock for the production of carbonaceous porous materials for environmental applications such as CO_2 adsorption.

Declaration of Competing Interest

The authors declare that they have no known competing financial interests or personal relationships that could have appeared to influence the work reported in this paper.

Acknowledgments

This work has received funding from the project PID2019-108826RB-I00/SRA (State Research Agency)/10.13039/501100011033 and the project B-RNM-78-UGR20 (FEDER/Junta de Andalucía-Consejería de Transformación Económica, Industria, Conocimiento y Universidades). Also, the authors are grateful for the supporting analyses provided by the external services of the University of Granada (CIC) and the University of Málaga (SCAI). Funding for open access charge: Universidad de Granada / CBUA.

References

Adibfar, M., Kaghazchi, T., Asasian, N., Soleimani, M., 2014. Conversion of poly (ethylene terephthalate) waste into activated carbon: chemical activation and characterization. Chem. Eng. Technol. 37, 979–986. https://doi.org/10.1002/CEAT.201200719.

Almazán-Almazán, M.C., Pérez-Mendoza, M., López-Domingo, F.J., Fernández-Morales, I., Domingo-García, M., López-Garzón, F.J., 2007. A new method to obtain microporous carbons from PET: characterisation by adsorption and molecular simulation. Microporous Mesoporous Mater. 106, 219–228. https://doi.org/10.1016/J.MICROMESO.2007.02.053.

Al-Salem, S.M., Yang, Y., Wang, J., Leeke, G.A., 2020. Pyro-oil and wax recovery from reclaimed plastic waste in a continuous auger pyrolysis reactor. Energies 13, 2040. https://doi.org/10.3390/EN13082040.

Bedin, K.C., Martins, A.C., Cazetta, A.L., Pezoti, O., Almeida, V.C., 2016. KOH-activated carbon prepared from sucrose spherical carbon: adsorption equilibrium, kinetic and thermodynamic studies for Methylene Blue removal. Chem. Eng. J. 286, 476–484. https://doi.org/10.1016/J.CEJ.2015.10.099.

Cabernard, L., Pfister, S., Oberschelp, C., Hellweg, S., 2021. Growing environmental footprint of plastics driven by coal combustion, 2021 5:2 5 Nat. Sustain. 139–148. https://doi.org/10.1038/s41893-021-00807-2.

Cansado, I.P. da P., Mourão, P.A.M., Nabais, J.M.V., Tita, B., Batista, T., Rocha, T., Borges, C., Matos, G., 2022. Use of dirty plastic waste as precursors for activated

carbon production—a contribution to the circular economy. Water Environ. J. 36, 96–104. https://doi.org/10.1111/WEJ.12762.
Chao-Hsiung, W., Ching-Yuan, C., Jwo-Luen, H., Shin-Min, S., Leo-Wang, C., Feng-Wen, C., 1993. On the thermal treatment of plastic mixtures of MSW: pyrolysis kinetics. Waste Manag. 13, 221–235. https://doi.org/10.1016/0956-053X(93)90046-Y.
Chen, H., Wan, K., Zhang, Y., Wang, Y., 2021. Waste to wealth: chemical recycling and chemical upcycling of waste plastics for a great future. ChemSusChem 14, 4123–4136. https://doi.org/10.1002/CSSC.202100652.
Chen, W., Gong, M., Li, K., Xia, M., Chen, Z., Xiao, H., Fang, Y., Chen, Y., Yang, H., Chen, H., 2020. Insight into KOH activation mechanism during biomass pyrolysis: chemical reactions between O-containing groups and KOH. Appl. Energy 278, 115730. https://doi.org/10.1016/J.APENERGY.2020.115730.
Duranoğlu, D., Beker, Ü., 2012. Steam and KOH activated carbons from peach stones. Energy Sources, Part A: Recovery Util. Environ. Eff. 34, 1004–1015. https://doi.org/10.1080/15567036.2010.527910.
European Comission, n.d. A European Green Deal [WWW Document]. URL ⟨https://ec.europa.eu/info/strategy/priorities-2019–2024/european-green-deal_en⟩ (accessed 6.8.22).
Ge, C., Song, J., Qin, Z., Wang, J., Fan, W., 2016. Polyurethane foam-based ultramicroporous carbons for CO_2 capture. ACS Appl. Mater. Interfaces 8, 18849–18859. https://doi.org/10.1021/ACSAMI.6B04771.
Ge, C., Lian, D., Cui, S., Gao, J., Lu, J., 2019. Highly selective CO_2 capture on waste polyurethane foam-based activated carbon. Processes 7, 592. https://doi.org/10.3390/PR7090592.
Guo, T., Fan, Z., Du, Y., Xu, J., Kong, L., Pan, Y., Xiao, H., Xie, Q., 2021. Thermodynamics of CO_2 adsorption on cellulose-derived biochar prepared in ionic liquid. Can. J. Chem. Eng. 99, 1940–1961. https://doi.org/10.1002/CJCE.23940.
Hoseinzadeh Hesas, R., Arami-Niya, A., Wan Daud, W.M.A., Sahu, J.N., 2015. Microwave-assisted production of activated carbons from oil palm shell in the presence of CO_2 or N_2 for CO_2 adsorption. J. Ind. Eng. Chem. 24, 196–205. https://doi.org/10.1016/J.JIEC.2014.09.029.
Idrees, M., Rangari, V., Jeelani, S., 2018. Sustainable packaging waste-derived activated carbon for carbon dioxide capture. J. CO_2 Util. 26, 380–387. https://doi.org/10.1016/J.JCOU.2018.05.016.
Jaafar, Y., Abdelouahed, L., Hage, R., el, Samrani, A., el, Taouk, B., 2022. Pyrolysis of common plastics and their mixtures to produce valuable petroleum-like products. Polym. Degrad. Stab. 195, 109770 https://doi.org/10.1016/J.POLYMDEGRADSTAB.2021.109770.
Kaur, B., Gupta, R.K., Bhunia, H., 2019a. Chemically activated nanoporous carbon adsorbents from waste plastic for CO_2 capture: Breakthrough adsorption study. Microporous Mesoporous Mater. 282, 146–158. https://doi.org/10.1016/J.MICROMESO.2019.03.025.
Kaur, B., Singh, J., Gupta, R.K., Bhunia, H., 2019b. Porous carbons derived from polyethylene terephthalate (PET) waste for CO_2 capture studies. J. Environ. Manag. 242, 68–80. https://doi.org/10.1016/J.JENVMAN.2019.04.077.
Kozyatnyk, I., Oesterle, P., Wurzer, C., Mašek, O., Jansson, S., 2021. Removal of contaminants of emerging concern from multicomponent systems using carbon dioxide activated biochar from lignocellulosic feedstocks. Bioresour. Technol. 340, 125561 https://doi.org/10.1016/J.BIORTECH.2021.125561.
Leal Filho, W., Saari, U., Fedoruk, M., Iital, A., Moora, H., Klöga, M., Voronova, V., 2019. An overview of the problems posed by plastic products and the role of extended producer responsibility in Europe. J. Clean. Prod. 214, 550–558. https://doi.org/10.1016/J.JCLEPRO.2018.12.256.
Li, Kunlin, Li, Kai, Wang, C., Ning, P., Sun, X., Song, X., Wang, Y., 2020. Preparation of polyacrylonitrile-based activated carbon fiber for CS_2 adsorption. Res. Chem. Intermed. 46, 3459–3476. https://doi.org/10.1007/S11164-020-04156-1/FIGURES/11.
Lillo-Ródenas, M.A., Cazorla-Amorós, D., Linares-Solano, A., 2003. Understanding chemical reactions between carbons and NaOH and KOH: An insight into the chemical activation mechanism. Carbon 41, 267–275. https://doi.org/10.1016/S0008-6223(02)00279-8.
Martín-Lara, M.A., Piñar, A., Ligero, A., Blázquez, G., Calero, M., 2021. Characterization and use of char produced from pyrolysis of post-consumer mixed plastic waste. Water 13, 1188. https://doi.org/10.3390/W13091188.
Masry, M., Rossignol, S., Gardette, J.L., Therias, S., Bussière, P.O., Wong-Wah-Chung, P., 2021. Characteristics, fate, and impact of marine plastic debris exposed to sunlight: a review. Mar. Pollut. Bull. 171, 112701 https://doi.org/10.1016/J.MARPOLBUL.2021.112701.
Mofijur, M., Ahmed, S.F., Rahman, S.M.A., Arafat Siddiki, S.Y., Islam, A.B.M.S., Shahabuddin, M., Ong, H.C., Mahlia, T.M.I., Djavanroodi, F., Show, P.L., 2021. Source, distribution and emerging threat of micro- and nanoplastics to marine organism and human health: Socio-economic impact and management strategies. Environ. Res. 195, 110857 https://doi.org/10.1016/J.ENVRES.2021.110857.
Panahi, S., Sardarian, A.R., Esmaeilzadeh, F., Almoneef, M.M., Jedli, H., Mbarek, M., 2021. Experimental study of CO_2 adsorption using activated carbon. Mater. Res Express 8, 065602. https://doi.org/10.1088/2053-1591/AC05FE.
Park, S.J., Jung, W.Y., 2002. Effect of KOH activation on the formation of oxygen structure in activated carbons synthesized from polymeric precursor. J. Colloid Interface Sci. 250, 93–98. https://doi.org/10.1006/JCIS.2002.8309.
Plastics Europe, 2021. Plastics - the Facts 2021 [WWW Document]. URL ⟨https://plasticseurope.org/knowledge-hub/plastics-the-facts-2021/⟩ (accessed 4.11.22).
Rashidi, N.A., Bokhari, A., Yusup, S., 2021. Evaluation of kinetics and mechanism properties of CO_2 adsorption onto the palm kernel shell activated carbon. Environ. Sci. Pollut. Res. 28, 33967–33979. https://doi.org/10.1007/S11356-020-08823-Z.
Santos, B.P.S., Almeida, D., Marques, M., de, F.V., Henriques, C.A., 2018. Petrochemical feedstock from pyrolysis of waste polyethylene and polypropylene using different catalysts. Fuel 215, 515–521. https://doi.org/10.1016/J.FUEL.2017.11.104.
Shi, S., Liu, Y., 2021. Nitrogen-doped activated carbons derived from microalgae pyrolysis by-products by microwave/KOH activation for CO_2 adsorption. Fuel 306, 121762. https://doi.org/10.1016/J.FUEL.2021.121762.
Singh, J., Bhunia, H., Basu, S., 2019. Adsorption of CO_2 on KOH activated carbon adsorbents: effect of different mass ratios. J. Environ. Manag. 250, 109457 https://doi.org/10.1016/J.JENVMAN.2019.109457.
Solis, M., Silveira, S., 2020. Technologies for chemical recycling of household plastics – a technical review and TRL assessment. Waste Manag. 105, 128–138. https://doi.org/10.1016/J.WASMAN.2020.01.038.
Thiounn, T., Smith, R.C., 2020. Advances and approaches for chemical recycling of plastic waste. J. Polym. Sci. 58, 1347–1364. https://doi.org/10.1002/POL.20190261.
Tseng, R.L., 2006. Mesopore control of high surface area NaOH-activated carbon. J. Colloid Interface Sci. 303, 494–502. https://doi.org/10.1016/J.JCIS.2006.08.024.
Wang, J., Liu, T.L., Huang, Q.X., Ma, Z.Y., Chi, Y., Yan, J.H., 2017. Production and characterization of high quality activated carbon from oily sludge. Fuel Process. Technol. 162, 13–19. https://doi.org/10.1016/J.FUPROC.2017.03.017.
Williams, P.T., Slaney, E., 2007. Analysis of products from the pyrolysis and liquefaction of single plastics and waste plastic mixtures. Resour. Conserv. Recycl. 51, 754–769. https://doi.org/10.1016/J.RESCONREC.2006.12.002.
Williams, P.T., Williams, E.A., 1998. Interaction of plastics in mixed-plastics pyrolysis. Energy Fuels 13, 188–196. https://doi.org/10.1021/EF980163X.
Wu, R., Ye, Q., Wu, K., Wang, L., Dai, H., 2021. Highly efficient CO_2 adsorption of corn kernel-derived porous carbon with abundant oxygen functional groups. J. CO_2 Util. 51, 101620 https://doi.org/10.1016/J.JCOU.2021.101620.
Yuan, X., Lee, J.G., Yun, H., Deng, S., Kim, Y.J., Lee, J.E., Kwak, S.K., Lee, K.B., 2020. Solving two environmental issues simultaneously: Waste polyethylene terephthalate plastic bottle-derived microporous carbons for capturing CO_2. Chem. Eng. J. 397, 125350 https://doi.org/10.1016/J.CEJ.2020.125350.
Zhang, R., Dai, Q., You, Z., Wang, H., Peng, C., 2018. Rheological performance of bio-char modified asphalt with different particle sizes, 1665 8 Appl. Sci. 2018 Vol. 8, 1665. https://doi.org/10.3390/APP8091665.
Zhang, Y., Ji, G., Chen, C., Wang, Y., Wang, W., Li, A., 2020. Liquid oils produced from pyrolysis of plastic wastes with heat carrier in rotary kiln. Fuel Process. Technol. 206, 106455 https://doi.org/10.1016/J.FUPROC.2020.106455.
Zhang, Z., Xu, M., Wang, H., Li, Z., 2010. Enhancement of CO_2 adsorption on high surface area activated carbon modified by N_2, H_2 and ammonia. Chem. Eng. J. 160, 571–577. https://doi.org/10.1016/J.CEJ.2010.03.070.
Zhao, S., Huang, B., Ye, X.P., Shu, X., Jia, X., 2014. Utilizing bio-char as a bio-modifier for asphalt cement:a sustainable application of bio-fuel by-product. Fuel 133, 52–62. https://doi.org/10.1016/J.FUEL.2014.05.002.